Acta Cryst E CRYSTALLOGRAPHIC COMMUNICATIONS

ISSN 2056-9890

Crystal structure of hydrazine iron(III) phosphate, the first transition metal phosphate containing hydrazine

Renald David

Laboratoire de Réactivité et Chimie des Solides (LRCS), Université de Picardie Jules Verne, CNRS UMR 7314, 33 rue Saint Leu, 80039 Amiens, France. *Correspondence e-mail: renald.david@u-picardie.fr

Received 7 October 2015
Accepted 22 October 2015

Edited by M. Weil, Vienna University of Technology, Austria

Keywords: crystal structure; hydrazine; iron phosphate; isotypism

CCDC reference: 1432700
Supporting information: this article has supporting information at journals.iucr.org/e

The title compound, poly[(μ_2-hydrazine)(μ_4-phosphato)iron(III)], [Fe(PO_4)(N_2H_4)]$_n$, was prepared under hydrothermal conditions. Its asymmetric unit contains one Fe^{III} atom located on an inversion centre, one P atom located on a twofold rotation axis, and two O, one N and two H atoms located on general positions. The Fe^{III} atom is bound to four O atoms of symmetry-related PO_4 tetrahedra and to two N atoms of two symmetry-related hydrazine ligands, resulting in a slightly distorted FeO_4N_2 octahedron. The crystal structure consists of a three-dimensional hydrazine/iron phoshate framework whereby each PO_4 tetrahedron bridges four Fe^{III} atoms and each hydrazine ligand bridges two Fe^{III} atoms. The H atoms of the hydrazine ligands are also involved in moderate N—H···O hydrogen bonding with phosphate O atoms. The crystal structure is isotypic with the sulfates [Co(SO_4)(N_2H_4)] and [Mn(SO_4)(N_2H_4)].

1. Chemical context

During the last century, transition metal phosphates have been studied intensively not only for their rich crystal- and magneto-chemistry (Kabbour *et al.*, 2012), but also for their various potential applications. For example, $NH_4M^{II}PO_4{\cdot}H_2O$ phases, where M is a transition metal, are used as pigments for protective paint finishes on metals, as fire retardants in paints

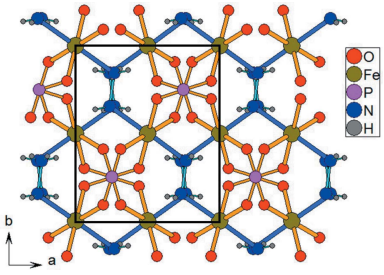

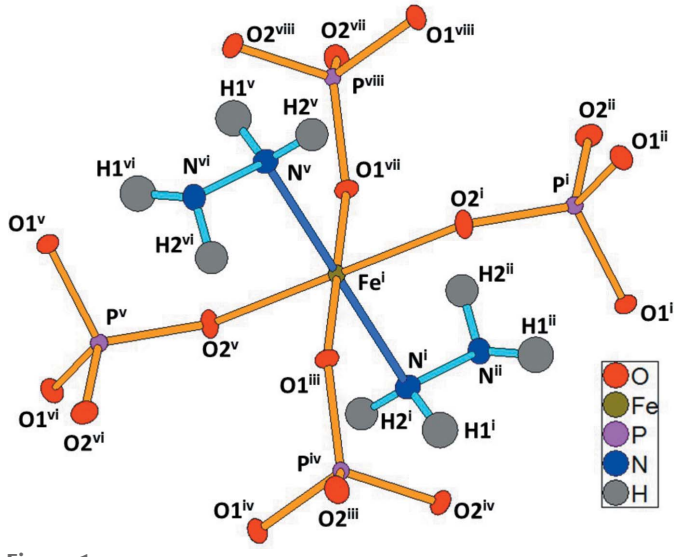

Figure 1
The coordination environment of the Fe^{III} atom in the structure of [Fe(PO_4)(N_2H_4)]. Displacement ellipsoids are drawn at the 50% probability level. [Symmetry codes: (i) x, y, z; (ii) 0.5-x, 0.5-y; (iii) $-x$, y + 0.5, 0.5-z; (iv) x + 0.5, $-y$, 0.5-z; (v) $-x$, $-y$, $-z$; (vi) x + 0.5, y + 0.5, $-z$; (vii) x, 0.5-y, z + 0.5; (viii) 0.5-x, y, z + 0.5.]

Table 1
Hydrogen-bond geometry (Å, °).

D—H···A	D—H	H···A	D···A	D—H···A
N—H1···O1^{i}	0.85 (3)	2.36 (2)	3.086 (2)	144 (2)
N—H1···O2^{ii}	0.85 (3)	2.27 (3)	2.974 (2)	141 (2)
N—H2···O1^{iii}	0.85 (3)	2.19 (3)	2.873 (2)	137 (2)

Symmetry codes: (i) $-x+\frac{1}{2}, -y+\frac{1}{2}, z$; (ii) $x+\frac{1}{2}, -y, -z+\frac{1}{2}$; (iii) $-x+\frac{1}{2}, y, z-\frac{1}{2}$.

and plastics but may also be applied as catalysts, fertilizers and magnetic devices (Erskine *et al.*, 1944; Bridger *et al.*, 1962; Barros *et al.*, 2006; Ramajo *et al.*, 2009). More recently, it was demonstrated by Goodenough and co-workers that in electrodes the presence of PO_4 groups results in higher positive potentials (Padhi *et al.*, 1997), leading to an intensive research on $LiFePO_4$, one of the most promising materials for the new generation of Li batteries (Ouvrard *et al.*, 2013).

2. Structural commentary

The structure of the title compound, $[Fe(PO_4)(N_2H_4)]$, is isotypic with the sulfates $[Co(SO_4)(N_2H_4)]$ and $[Mn(SO_4)(N_2H_4)]$ (Jia *et al.*, 2011). The Fe^{III} atom is bound to four PO_4 tetrahedra and to two N atoms of hydrazine ligands, resulting in a slightly distorted FeO_4N_2 octahedron (Fig. 1). The crystal structure consists of a three-dimensional network made up of Fe^{III} atoms which are interconnected through neutral hydrazine (N_2H_4) ligands and phosphate (PO_4^{3-}) anions (Fig. 2). If the phosphate and sulfate structures are isotypic, the presence of phosphate implies an oxidation state of +III for the transition metal compared to +II for the sulfate analogues. The replacement of sulfate for phosphate leads to a change in the coordination sphere of the metal. These differences are mainly associated with the metal–oxygen bond lengths. The average Fe^{III}—O bond length is 1.97 Å for $[Fe(PO_4)(N_2H_4)]$ and the average Co^{II}—O bond length is 2.12 Å for $[Co(SO_4)(N_2H_4)]$, whereas the average M—N bond lengths involving the N atom of the hydrazine ligand are similar, with values of 2.17 and 2.12 Å, respectively. As a consequence, the FeN_2O_4 octahedron is more distorted, appearing like an FeO_4 square additionally bound by two *trans* hydrazine ligands in axial positions.

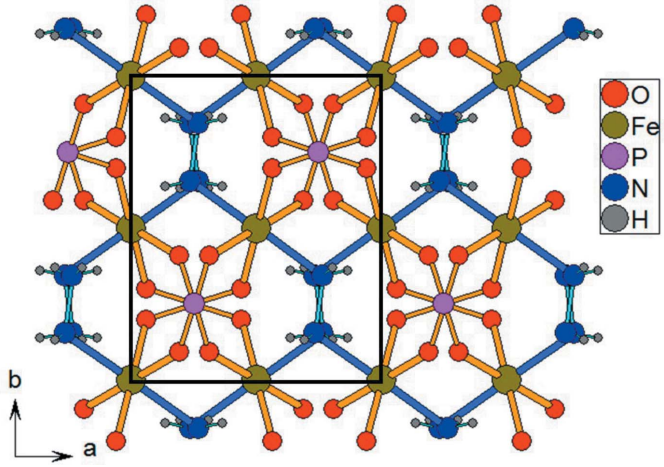

Figure 2
The crystal structure of $[Fe(PO_4)(N_2H_4)]$ in a projection along [001].

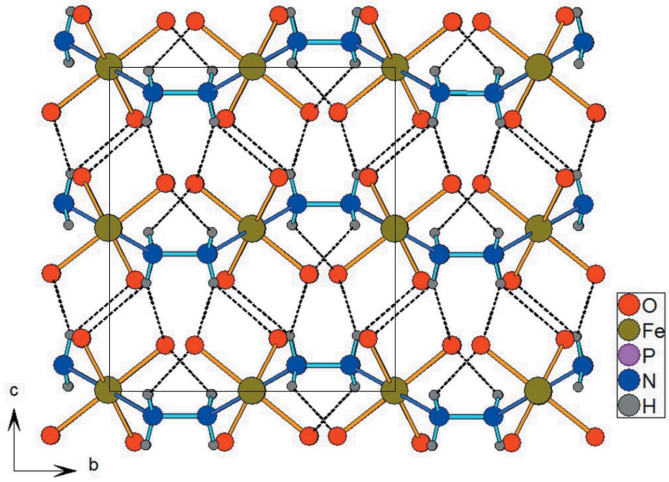

Figure 3
The crystal structure of $[Fe(PO_4)(N_2H_4)]$ in a projection along [100], emphasizing the hydrogen bonding between the components (black dotted lines). P atoms have been omitted for clarity.

It should be noted that it seems rather surprising to stabilize Fe^{III} with hydrazine, since the latter is a powerful reducing agent. Efforts are currently underway to obtain the title compound as a pure phase to perform magnetic measurements. It could be a way, by comparison with the results reported for $[Co(SO_4)(N_2H_4)]$ (Jia *et al.*, 2011), to study the ability of hydrazine to transmit magnetic coupling.

3. Supramolecular features

The three-dimensional framework structure of $[Fe(PO_4)(N_2H_4)]$ is consolidated by N—H···O interactions between the hydrazine ligands and phosphate O atoms (Fig. 3). One of the two hydrogen bonds is bifurcated. Considering the N···O distances and the values of the N—H···angles (Table 1), this type of hydrogen bonding can be considered as moderately strong.

4. Synthesis and crystallization

Iron(II) chloride tetrahydrate (>99.0%, Sigma–Aldrich), hydrazine monohydrate (99+%) and KH_2PO_4 (both VWR International) were used as received without further purification. Iron(II) chloride tetrahydrate (2 g) was dissolved in water (20 ml) before adding hydrazine monohydrate (2 ml). The obtained solution was stirred for 5 min. Then, KH_2PO_4 (11.5 g) was added. After 10 min of stirring for homogenization, the obtained solution (15 ml) was incorporated in a 23 ml autoclave. The autoclave was then heated at 433 K for 10 h before being cooled to room temperature at a rate of 10 K h^{-1}. The obtained mixture, consiting of orange crystals of the title phase and yellow crystals of an additional phase, was washed with water. The obtained crystals were very small

(around 20 μm) and well isolated from the others. Details of the composition and structure of the yellow crystals will be described in a forthcoming article.

5. Refinement details

Crystal data, data collection and structure refinements are summarized in Table 2. All H atoms were located in a difference Fourier map and were refined freely with isotropic displacement parameters.

Acknowledgements

The RS2E (French Network on Electrochemical Energy Storage) and ANR (Labex STORE-EX; grant No. ANR-10-LABX-0076) are acknowledged for funding of the X-ray diffractometer.

Table 2
Experimental details.

Crystal data	
Chemical formula	$[Fe(PO_4)(N_2H_4)]$
M_r	182.87
Crystal system, space group	Orthorhombic, *Pccn*
Temperature (K)	293
a, *b*, *c* (Å)	6.3114 (13), 7.6680 (15), 8.6485 (18)
V (Å^3)	418.55 (15)
Z	4
Radiation type	Mo $K\alpha$
μ (mm^{-1})	3.89
Crystal size (mm)	0.05 × 0.03 × 0.03
Data collection	
Diffractometer	Bruker APEXII CCD
Absorption correction	Multi-scan (*SADABS*; Bruker, 2013)
T_{min}, T_{max}	0.668, 0.746
No. of measured, independent and observed [$I > 3\sigma(I)$] reflections	13820, 601, 457
R_{int}	0.065
$(\sin \theta/\lambda)_{max}$ (Å^{-1})	0.717
Refinement	
$R[F^2 > 3\sigma(F^2)]$, $wR(F^2)$, S	0.020, 0.027, 1.46
No. of reflections	601
No. of parameters	47
H-atom treatment	All H-atom parameters refined
$\Delta\rho_{max}$, $\Delta\rho_{min}$ (e Å^{-3})	0.40, −0.33

Computer programs: *APEX2*and *SAINT* (Bruker, 2013), *SUPERFLIP* (Palatinus & Chapuis, 2007), *JANA2006* (Petříček *et al.*, 2014) and *DIAMOND* (Brandenburg & Putz, 2010).

References

Barros, N., Airoldi, C., Simoni, J. A., Ramajo, B., Espina, A. & García, J. R. (2006). *Thermochim. Acta*, **441**, 89–95.
Brandenburg, K. & Putz, H. (2010). *DIAMOND*. Crystal Impact GbR, Bonn, Germany.
Bridger, G. L., Salutsky, M. L. & Starostka, R. W. (1962). *J. Agric. Food Chem.* **10**, 181–188.
Bruker (2013). *APEX2*, *SAINT* and *SADABS*. Bruker–Nonius AXS Inc., Madison, Wisconsin, USA.
Erskine, A. M., Grimm, G. & Horning, S. C. (1944). *Ind. Eng. Chem.* **36**, 456–460.
Jia, L.-H., Li, R.-Y., Duan, Z.-M., Jiang, S.-D., Wang, B.-W., Wang, Z.-M. & Gao, S. (2011). *Inorg. Chem.* **50**, 144–154.
Kabbour, H., David, R., Pautrat, A., Koo, H.-J., Whangbo, M.-H., André, G. & Mentré, O. (2012). *Angew. Chem. Int. Ed.* **51**, 11745–11749.
Ouvrard, G., Zerrouki, M., Soudan, P., Lestriez, B., Masquelier, C., Morcrette, M., Hamelet, S., Belin, S., Flank, A. M. & Baudelet, F. (2013). *J. Power Sources*, **229**, 16–21.
Padhi, A. K., Nanjundaswamy, K. S., Masquelier, C., Okada, S. & Goodenough, J. B. (1997). *J. Electrochem. Soc.* **144**, 1609–1613.
Palatinus, L. & Chapuis, G. (2007). *J. Appl. Cryst.* **40**, 786–790.
Petříček, V., Dušek, M. & Palatinus, L. (2014). *Z. Kristallogr.* **229**, 345–352.
Ramajo, B., Espina, A., Barros, N. & García, J. R. (2009). *Thermochim. Acta*, **487**, 60–64.

supporting information

Acta Cryst. (2015). E**71**, 1436-1438 [https://doi.org/10.1107/S2056989015020010]

Crystal structure of hydrazine iron(III) phosphate, the first transition metal phosphate containing hydrazine

Renald David

Computing details

Data collection: *APEX2* (Bruker, 2013); cell refinement: *SAINT* (Bruker, 2013); data reduction: *SAINT* (Bruker, 2013); program(s) used to solve structure: SUPERFLIP (Palatinus & Chapuis, 2007); program(s) used to refine structure: JANA2006 (Petříček *et al.*, 2014); molecular graphics: *DIAMOND* (Brandenburg & Putz, 2010); software used to prepare material for publication: JANA2006 (Petříček *et al.*, 2014).

Poly[(μ_2-hydrazine)(μ_4-phosphato)iron(III)]

Crystal data

$[Fe(PO_4)(N_2H_4)]$
$M_r = 182.87$
Orthorhombic, *Pccn*
Hall symbol: -P 2ab 2ac
$a = 6.3114\ (13)$ Å
$b = 7.6680\ (15)$ Å
$c = 8.6485\ (18)$ Å
$V = 418.55\ (15)$ Å^3
$Z = 4$
$F(000) = 364$
$D_x = 2.902$ Mg m^{-3}
Mo $K\alpha$ radiation, $\lambda = 0.71073$ Å
Cell parameters from 2128 reflections
$\theta = 4.2–26.9°$
$\mu = 3.89$ mm^{-1}
$T = 293$ K
Parallelepiped, orange
0.05 × 0.03 × 0.03 mm

Data collection

Bruker APEXII CCD diffractometer
Radiation source: X-ray tube
phi scan
Absorption correction: multi-scan (*SADABS*; Bruker, 2013)
$T_{min} = 0.668$, $T_{max} = 0.746$
13820 measured reflections
601 independent reflections
457 reflections with $I > 3\sigma(I)$
$R_{int} = 0.065$
$\theta_{max} = 30.6°$, $\theta_{min} = 4.2°$
$h = -9\rightarrow8$
$k = -10\rightarrow10$
$l = -12\rightarrow12$

Refinement

Refinement on F
$R[F > 3\sigma(F)] = 0.020$
$wR(F) = 0.027$
$S = 1.46$
601 reflections
47 parameters
0 restraints
0 constraints
All H-atom parameters refined
Weighting scheme based on measured s.u.'s $w = 1/(\sigma^2(F) + 0.0001F^2)$
$(\Delta/\sigma)_{max} = 0.006$
$\Delta\rho_{max} = 0.40$ e Å^{-3}
$\Delta\rho_{min} = -0.33$ e Å^{-3}

Fractional atomic coordinates and isotropic or equivalent isotropic displacement parameters (Å²)

	x	*y*	*z*	U_{iso}*/U_{eq}
O1	−0.0604 (2)	0.30096 (17)	0.36016 (16)	0.0093 (4)
Fe	0	0	0	0.00652 (11)
P	−0.25	0.25	0.25868 (8)	0.00567 (17)
O2	−0.1898 (2)	0.09269 (19)	0.15978 (16)	0.0111 (4)
N	0.2656 (3)	0.1556 (2)	0.0781 (2)	0.0103 (5)
H1	0.306 (4)	0.132 (3)	0.169 (3)	0.024 (7)*
H2	0.364 (4)	0.139 (3)	0.012 (3)	0.020 (7)*

Atomic displacement parameters (Å²)

	U^{11}	U^{22}	U^{33}	U^{12}	U^{13}	U^{23}
O1	0.0089 (6)	0.0090 (7)	0.0099 (7)	0.0001 (5)	−0.0032 (5)	−0.0013 (5)
Fe	0.00692 (19)	0.0059 (2)	0.00678 (19)	−0.00013 (13)	0.00010 (16)	−0.00054 (16)
P	0.0059 (3)	0.0053 (3)	0.0057 (3)	−0.0001 (3)	0	0
O2	0.0135 (6)	0.0096 (7)	0.0101 (7)	0.0003 (5)	0.0030 (6)	−0.0033 (6)
N	0.0110 (8)	0.0074 (8)	0.0123 (9)	−0.0017 (7)	−0.0012 (8)	0.0010 (7)

Geometric parameters (Å, º)

O1—Fe^{i}	1.9843 (14)	P—O2^{iii}	1.5268 (15)
O1—P	1.5346 (15)	N—N^{iv}	1.461 (2)
Fe—O2	1.9621 (15)	N—H1	0.85 (3)
Fe—O2^{ii}	1.9621 (15)	N—H2	0.85 (3)
P—O2	1.5268 (15)		
Fe^{i}—O1—P	133.97 (8)	O1—P—O2^{iii}	108.25 (7)
O1^{v}—Fe—O1^{vi}	180.0 (5)	O1^{iii}—P—O2	108.25 (7)
O1^{v}—Fe—O2	88.09 (6)	O1^{iii}—P—O2^{iii}	109.13 (7)
O1^{v}—Fe—O2^{ii}	91.91 (6)	O2—P—O2^{iii}	111.85 (9)
O1^{vi}—Fe—O2	91.91 (6)	Fe—O2—P	146.37 (9)
O1^{vi}—Fe—O2^{ii}	88.09 (6)	N^{iv}—N—H1	104.6 (18)
O2—Fe—O2^{ii}	180.0 (5)	N^{iv}—N—H2	104.2 (18)
O1—P—O1^{iii}	110.23 (8)	H1—N—H2	112 (2)
O1—P—O2	109.13 (7)		

Symmetry codes: (i) −*x*, *y*+1/2, −*z*+1/2; (ii) −*x*, −*y*, −*z*; (iii) −*x*−1/2, −*y*+1/2, *z*; (iv) −*x*+1/2, −*y*+1/2, *z*; (v) −*x*, *y*−1/2, −*z*+1/2; (vi) *x*, −*y*+1/2, *z*−1/2.

Hydrogen-bond geometry (Å, º)

D—H···*A*	*D*—H	H···*A*	*D*···*A*	*D*—H···*A*
N—H1···O1^{iv}	0.85 (3)	2.36 (2)	3.086 (2)	144 (2)
N—H1···O2^{vii}	0.85 (3)	2.27 (3)	2.974 (2)	141 (2)
N—H2···O1^{viii}	0.85 (3)	2.19 (3)	2.873 (2)	137 (2)

Symmetry codes: (iv) −*x*+1/2, −*y*+1/2, *z*; (vii) *x*+1/2, −*y*, −*z*+1/2; (viii) −*x*+1/2, *y*, *z*−1/2.